



**Joint Institute for Nuclear Research**  
**Introduction to Quantum Computing**

Final Report on the INTEREST Program

**Wave 6:** 14 February - 25 March

Student: Maria Zaneva  
*Technical University of Sofia, Bulgaria*

Supervisors: Dr. Mihai Dima, Prof. Gheorghe Adam  
*Laboratory of Information Technologies*

Date: 26.03.2022

## **Abstract**

The project "Introduction to Quantum Computing" covered key concepts in the physics of quantum computations. Basic principles of quantum mechanics were discussed - spin properties and two-level systems, superposition, entanglement and interference phenomena. In this work, a brief summary of the theory is given. The graphical representation of the qubit states (Bloch sphere) is discussed as well as some of the Quantum Logic Gates. A brief introduction to the theory behind the superconducting phenomena, the Josephson effect and Transmon qubits are covered. Finally, the results from the qubit experiments using the IBM Quantum Lab are presented.

# Contents

<b>1</b>	<b>Introduction</b>	<b>3</b>
<b>2</b>	<b>Spin Quantum Mechanics</b>	<b>3</b>
2.1	Stern-Gerlach Experiment	3
2.2	Bloch Sphere	5
<b>3</b>	<b>Superconducting qubits</b>	<b>6</b>
3.1	Josephson Effect	6
3.2	Cooper pair box	7
3.3	Transmon Qubits	8
<b>4</b>	<b>Quantum Gates</b>	<b>9</b>
<b>5</b>	<b>Qubit Measurements</b>	<b>11</b>
5.1	Qubit Frequency Scan	11
5.2	Rabi Oscillations. $\pi$ pulse	12
5.3	0/1 Discriminator	13
5.4	Relaxation time $T_1$	13
5.5	Ramsay Experiment. Precise Qubit Frequency	13
5.6	Hahn Echo Experiment. Measuring time $T_2$	14
5.7	Dynamical Decoupling	15
<b>6</b>	<b>Conclusions</b>	<b>15</b>

# 1 Introduction

Quantum computing is a tool that helps us satisfy the need of greater efficiency of computing power. This area of research studies how to incorporate the strange phenomena of physics from the twentieth century into computer science. The three key ideas of quantum mechanics – entanglement, superposition, and measurement, provide a new computational model for information processing.

A classical computer operates on strings of zeros and ones. Each position in such a string is called a bit and it is the basic unit of data. Each physical state is associated with a value of either zero or one.

Analogously, the basic unit of data for quantum computations is the quantum bit (qubit). A qubit can assume the logical values "0" or "1" similar to classical bits. However, it can also be in a logical state that contains any linear combination of them as shall be discussed in the next sections. Qubits can be entangled, in a superposition state or even interfere with each other, making them much more powerful than classical bits.

## 2 Spin Quantum Mechanics

### 2.1 Stern-Gerlach Experiment

The spin property of the electron was revealed in 1922 in the Stern-Gerlach experiment (Figure 1).

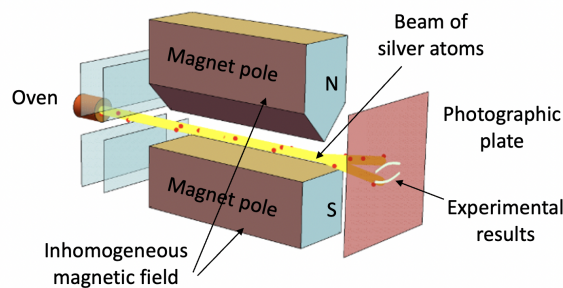


Figure 1: Stern-Gerlach Experiment. A beam of hot silver atoms shot through inhomogeneous magnetic field and landing on a photographic plate. The experimental results suggests that the division of the beam was due to the interaction of the spin with the magnetic field

A beam of hot silver atoms was shot through a pair of slits and an inhomogeneous magnetic field. Due to the neutrality of the silver atom no interaction with the magnetic field was expected, but the particles landed on the photographic plate creating a pattern of two lines. The division of the beam into two suggested that a quantum intrinsic angular momentum property of the electrons, known as spin, interacted with the magnetic field.

It turns out that the spin has a fundamental physical meaning. Depending on the spin, the particles fall into the two categories – fermions and bosons as shown below. While the fermions represent the building blocks of matter, bosons are the quanta of the fields that carry out the interactions – they acts as "glue" between the fundamental "blocks".

Every elementary particle has a specific and immutable value of the spin:

- Fermions:

$$s = \frac{1}{2}; \frac{3}{2}; \frac{5}{2}; \dots$$

- Bosons:

$$s = 0; 1; 2; \dots$$

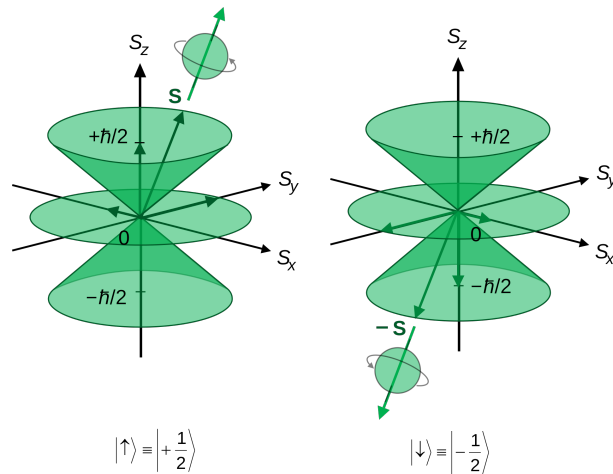


Figure 2: Spin Angular Momentum. The direction of intrinsic spin is quantized. For electrons:  $S_z = m_s \frac{\hbar}{2\pi}$ , ( $m_s = \pm \frac{1}{2}$ ) where  $S_z$  is the z-component of spin angular momentum and  $m_s$  is the spin projection quantum number. The spin projection is referred to as spin up ( $m_s = +\frac{1}{2}$ ) and spin down ( $m_s = -\frac{1}{2}$ )

By far, the most important case is  $s = \frac{1}{2}$ , for this is the spin of the particles that make up ordinary matter, as well as all quarks and all leptons. There are two eigenstates, which we call *spin up* and *spin down* (Figure 2). Those systems with only two possible states are known as **two-level (two-state) quantum systems**. [3]

The qubit model is considered to be a two-level system like the spin and we can think that their properties are analogous.

## 2.2 Bloch Sphere

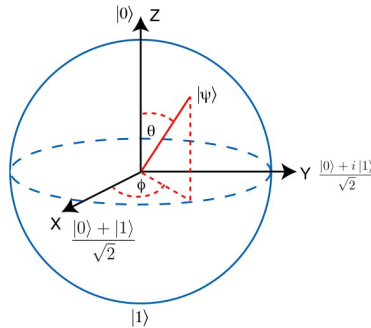


Figure 3: Bloch Sphere. Geometrical representation of the pure state of a two-level system. The north and the south poles are corresponding to the  $|0\rangle$  and  $|1\rangle$  basis vectors (spin-up and spin-down states). Any pure state  $\psi$  of a two-level system can be expressed as a superposition of the basis vectors  $|0\rangle$  and  $|1\rangle$ . The parameters  $\theta$  and  $\phi$  specify a point in the sphere that corresponds to a given pure state of the system  $\psi$  [7].

The eigenstates of a qubit are represented by  $|0\rangle$  and  $|1\rangle$  which are defined by the following two vectors:

$$|0\rangle = \begin{bmatrix} 1 \\ 0 \end{bmatrix}; |1\rangle = \begin{bmatrix} 0 \\ 1 \end{bmatrix}$$

As we have mentioned, the state of a qubit  $|\psi\rangle$  can also be represented by a linear combination of the two:

$$|\psi\rangle = \alpha |0\rangle + \beta e^{i\phi} |1\rangle; \quad \alpha, \beta \in \mathbb{R}, \quad \alpha^2 + \beta^2 = 1$$

After parametrization by the angles  $\theta$  and  $\phi$  the state is as follows:

$$|\psi\rangle = \cos\frac{\theta}{2} |0\rangle + \sin\frac{\theta}{2} e^{i\phi} |1\rangle$$

The Bloch Sphere is a graphical way to represent these two-level systems. It is a unit radius sphere and it allows a geometric visualization of the quantum state of the qubit as a point on its surface (Figure 3).

## 3 Superconducting qubits

### 3.1 Josephson Effect

Circuit quantum electrodynamics devices (QED) make use of the quantum dynamics of electromagnetic fields in superconducting circuits to process quantum information. These devices are usually formed by embedding a superconducting device, known as Josephson junction, into another system made of superconductors.

Superconductivity plays a very important role in the operation of all circuit QED systems. In superconductors the charge carriers are coupled electrons that form **Cooper pairs**. Each electron in a Cooper pair has equal and opposite spin and momentum.

The **Josephson junction** is a device in which two superconducting electrodes are separated by a thin insulator (*Figure 4*). It can be viewed as being synonymous to a nonlinear inductor. The phenomenon where an electric current is allowed to pass between the superconductors due to the coherent tunneling of Cooper pairs, is known as the **Josephson effect**.

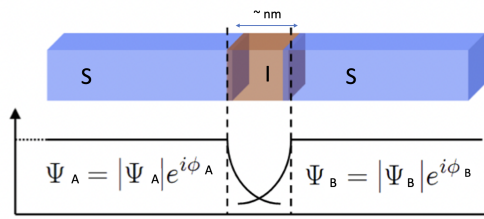


Figure 4: Schematic Diagram of a Josephson Junction [2]. Two superconducting electrodes (S) separated by a thin layer of insulator (I).  $\psi_A$  and  $\psi_B$  are macroscopic wave functions of Cooper pairs in the electrodes. A current flows through the junction as the Cooper pairs are able to tunnel through the thin insulator.

The order parameter at each electrode can be written as:

$$\Psi_A = |\Psi_A| e^{i\phi_A}; \quad \Psi_B = |\Psi_B| e^{i\phi_B} \quad (1)$$

Where  $\phi_{A(B)}$  are the macroscopic wave functions of Cooper pairs in the first and second electrodes.

The supercurrent  $I_S$ , flowing through the junction is related to the phase difference between the electrodes  $\phi$  and the critical current  $I_C$  as follows:

$$I_S = I_C \sin(\phi(t)), \quad \phi = \phi_A - \phi_B \quad (2)$$

The critical current,  $I_C = 2eE_J/\hbar$ , is the maximum current that the junction can carry without any dissipation and depends on the properties of the superconductors and  $E_J$  is the **Josephson energy**, which measures the energy of a Cooper pair tunneling through the junction.

Equation (2) is the **first Josephson relation** (current-phase relation). The **second Josephson relation** also known as the superconducting phase evolution equation is given by:

$$\frac{\partial \phi}{\partial t} = \frac{2eV(t)}{\hbar} \quad (3)$$

The Hamiltonian for the Josephson junction can be written as the sum of the inductive and capacitive energy:

$$H = H_C + H_L = 4E_C n^2 - E_J \cos \phi \quad (4)$$

### 3.2 Cooper pair box

The Cooper pair box (CPB) was one of the first qubits used to observe macroscopic quantum behaviour in circuit QED systems. The CPB consists of a Josephson junction that connects a superconducting island and reservoir (Figure 5a). The Hamiltonian is similar to Eq.(4),  $n_g$  - offset charge induced by the voltage source:

$$H = 4E_C (n - n_g)^2 - E_J \cos \phi, \quad (5)$$

In Figure 5b the diagram for the first three energy levels of a CPB as a function of  $n_g$  is shown. The frequencies of microwave radiation that can be emitted (or absorbed) is based on the energy difference between two adjacent energy levels. We observe that half-integer values for  $n_g$  are ideal for performing operations, because of the large gap between the first two excited states, and the energy levels are not evenly spaced. As a result of these properties, using fast microwave pulses, a transition between the ground and first excited state can be driven without the need of significant filtering of the pulse.

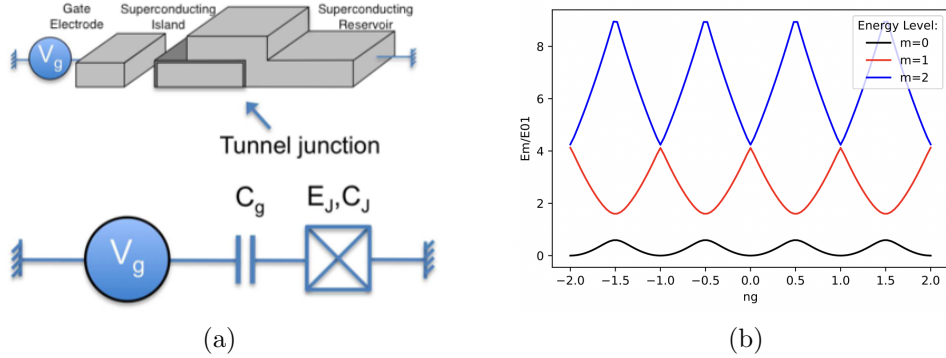


Figure 5: (a) Cooper Pair Box [6]. A superconducting island connected by a Josephson junction to a superconducting reservoir and capacitively coupled to a gate electrode. (b) First three energy levels for a qubit with a ratio of the Josephson energy  $E_J$  to the Charging energy  $E_C$  equal to one  $E_J/E_C = 1$ . The graphic is a function of the gate charge  $n_g = C_g \cdot V_g / 2e$ . Half-integer values for the gate charge  $n_g$  are the regions with the largest gap between the first two excited states, thus making them ideal for performing operations.

### 3.3 Transmon Qubits

The schematic of a transmon qubit is shown in Figure 6c. It is similar to the ordinary CPB and consists of two superconducting islands coupled through two Josephson junctions, but isolated from the rest of the circuit. The Hamiltonian is similar to the CPB system (Eq. 5), but due to the additional capacitance, the charging energy  $E_C$  can be made smaller than the Josephson energy  $E_J$ . As a result, the energy ratio  $E_J/E_C$  transitions from  $E_J/E_C < 1$  for CPB to  $E_J/E_C \gg 1$  for a transmon.

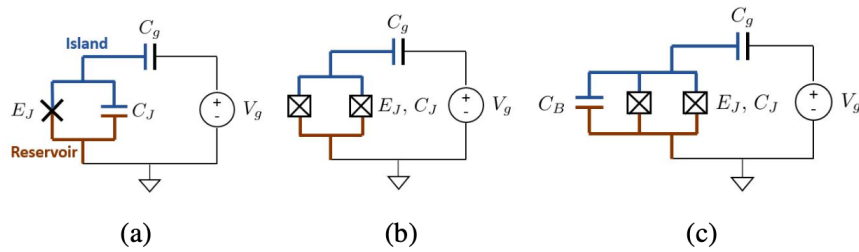


Figure 6: Schematics of (a) CPB, (b) split CPB, (c) transmon. The transmon consists of two superconducting islands coupled through Josephson junction and isolated from the rest of the circuit. The additional capacitance allows smaller values for the charging energy  $E_C$  and a transition to the energy ratio to  $E_J/E_C \gg 1$ , decreasing the charging dispersion.

In Figure 7b are shown the first three energy levels for different energy

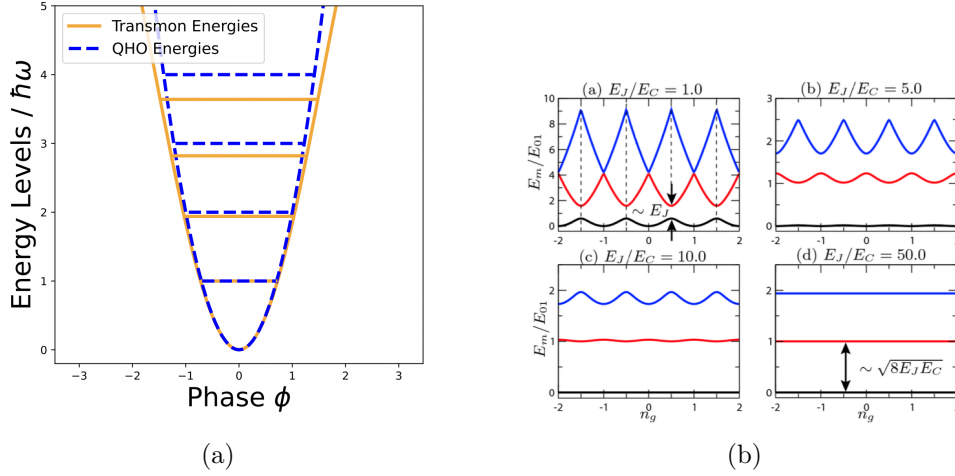


Figure 7: (a) Transmon energy levels (yellow) compared to QHO energies (blue). We can see that the transmon energy levels are anharmonic (not evenly spaced) which is why we can use it as a qubit opposing to the QHO. (b) First three energy levels for different  $E_J/E_C$  ratios [4]. A more stable qubit transition frequency with respect to noise is being observed with the increase of the ratio.

ratios. By increasing  $E_J/E_C$  an exponential decrease of the charging dispersion is observed and therefore a stable qubit transition frequency with respect to charge noise.

## 4 Quantum Gates

Claude Shannon showed that all boolean algebra could be performed using electrical switches. The combination of switches that correspond to the binary operators are called **gates**. A hardware quantum computer implements a core set of core gates and more advanced ones that are built from them using circuits. A **quantum circuit** is a sequence of gates that are applied to one or more qubits in a quantum register [1].

Figure 8 shows some of the quantum logic gates and their matrix representation:

- **The Pauli-X Gate:** The X Gate is equivalent of the NOT gate for classical computers and applying it means a rotation of the state of the qubit of 180 degrees. By looking at Fig. 3, we can observe that it can be visualized as a rotation around the X-axis;
- **The Pauli-Y Gate:** It is analogous to a rotation around the Y-axis of the Bloch sphere by  $\pi$  radians;

Operator	Gate(s)	Matrix
Pauli-X (X)	 $\oplus$	$\begin{bmatrix} 0 & 1 \\ 1 & 0 \end{bmatrix}$
Pauli-Y (Y)		$\begin{bmatrix} 0 & -i \\ i & 0 \end{bmatrix}$
Pauli-Z (Z)		$\begin{bmatrix} 1 & 0 \\ 0 & -1 \end{bmatrix}$
Hadamard (H)		$\frac{1}{\sqrt{2}} \begin{bmatrix} 1 & 1 \\ 1 & -1 \end{bmatrix}$
Phase (S, P)		$\begin{bmatrix} 1 & 0 \\ 0 & i \end{bmatrix}$
$\pi/8$ (T)		$\begin{bmatrix} 1 & 0 \\ 0 & e^{i\pi/4} \end{bmatrix}$
Controlled Not (CNOT, CX)		$\begin{bmatrix} 1 & 0 & 0 & 0 \\ 0 & 1 & 0 & 0 \\ 0 & 0 & 0 & 1 \\ 0 & 0 & 1 & 0 \end{bmatrix}$
Controlled Z (CZ)		$\begin{bmatrix} 1 & 0 & 0 & 0 \\ 0 & 1 & 0 & 0 \\ 0 & 0 & 1 & 0 \\ 0 & 0 & 0 & -1 \end{bmatrix}$
SWAP		$\begin{bmatrix} 1 & 0 & 0 & 0 \\ 0 & 0 & 1 & 0 \\ 0 & 1 & 0 & 0 \\ 0 & 0 & 0 & 1 \end{bmatrix}$
Toffoli (CCNOT, CCX, TOFF)		$\begin{bmatrix} 1 & 0 & 0 & 0 & 0 & 0 & 0 & 0 \\ 0 & 1 & 0 & 0 & 0 & 0 & 0 & 0 \\ 0 & 0 & 1 & 0 & 0 & 0 & 0 & 0 \\ 0 & 0 & 0 & 1 & 0 & 0 & 0 & 0 \\ 0 & 0 & 0 & 0 & 1 & 0 & 0 & 0 \\ 0 & 0 & 0 & 0 & 0 & 1 & 0 & 0 \\ 0 & 0 & 0 & 0 & 0 & 0 & 1 & 0 \\ 0 & 0 & 0 & 0 & 0 & 0 & 0 & 1 \end{bmatrix}$

Figure 8: Quantum Logic Gates and their matrix representation

- **The Pauli-Z Gate:** It equates to a rotation around the Z-axis of the Bloch sphere by  $\pi$  radians;
- **The Phase Gate:** The P gate performs a rotation of  $\phi$  around the Z-axis direction, where  $\phi$  is a real number. The Z-gate is a special case of the P-gate where  $\phi = \pi$ ;
- **Hadamard Gate:** The H-gate is a fundamental quantum gate. Applying it to a qubit brings the qubit to a superposition state;
- **CNOT Gate:** The Controlled-Not gate is analogous to the XOR gate in classical computing. It has two inputs and two outputs - it takes two qubits and thus it will be a 4x4 matrix. It leaves the control qubit unchanged and performs a Pauli-X gate on the target qubit when the control qubit is in state  $|1\rangle$  or leaves the target unchanged in case the control qubit is in state  $|0\rangle$ ;
- **SWAP Gate:** It is a two-qubit operation that when applied swaps their state;
- **Toffoli Gate:** Also known as the Controlled-Controlled NOT gate, it is a three qubit operation defined by the given in Figure 9 matrix:

## 5 Qubit Measurements

### 5.1 Qubit Frequency Scan

Using the IBM **Quantum Lab** in this exercise we are going to find the resonant frequency  $f_o$  of the qubit. This frequency is the difference in energy between the ground  $|0\rangle$  and excited states  $|1\rangle$ .

$$E_{01} = hf_{01}$$

It can be found by sweeping a frequency span (around 40MHz) and using a Network Analyzer with step of 1MHz in order to find signs of absorption. At each frequency a drive pulse, Gaussian pulse in our case, of that frequency will be sent to the qubit.

We fit the function to the data:

$$\frac{A}{\pi} \cdot \frac{B}{(x - q_{freq})^2 + b^2} + C \quad (6)$$

The peak in the center corresponds to the location of the qubit frequency (Figure 9):

$$f_{01} = 4.97167 \text{ GHz} \quad (7)$$

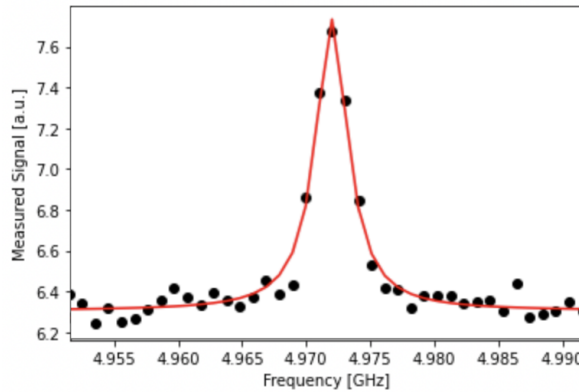


Figure 9: Qubit Frequency Scan. At each frequency from the chosen span a Gaussian drive pulse is being sent to the qubit. The resonant frequency of the qubit  $f_{01} = \frac{E_{01}}{h} = 4.97167 \text{ GHz}$  is found at the peak in the center after fitting (6) to the data.

## 5.2 Rabi Oscillations. $\pi$ pulse

The oscillations we see in *Figure 10* are called **Rabi Oscillations** and are a basic process used to manipulate qubits. They are obtained by exposing qubits to periodic electric or magnetic fields during adjusted time intervals. If at time  $t=0$  the qubit is in state  $|0\rangle$ , at time  $t$  it will have a probability  $p_{0\rightarrow 1}(t)$  of being found in the state  $|1\rangle$  [5]. At resonance, the oscillation between the states has maximum amplitude, where the frequency  $\omega_1$  is the *Rabi frequency*:

$$p_{0\rightarrow 1}(t) = \sin^2 \frac{\omega_1 t}{2}; \quad \frac{\omega_1 t}{2} = \frac{\pi}{2}, \quad t = \frac{\pi}{\omega_1}$$

The  $\pi$  pulse determines the transition between the two states of the qubit,  $|0\rangle$  and  $|1\rangle$  respectively. This is analogous to applying the X-gate and the rotation of the state on the Bloch sphere by  $\pi$  radians (Figure 10). We already know the microwave frequency needed to drive the transition from the previous experiment. To define the amplitude needed, we start with small pulses and increase their amplitudes progressively by measuring the state of the qubit at each step. The results were then fit into a curve given by the equation:

$$A \cos\left(\frac{2\pi x}{d} - \phi\right) + B \quad (8)$$

The  $\pi$  pulse amplitude is **0.15422**

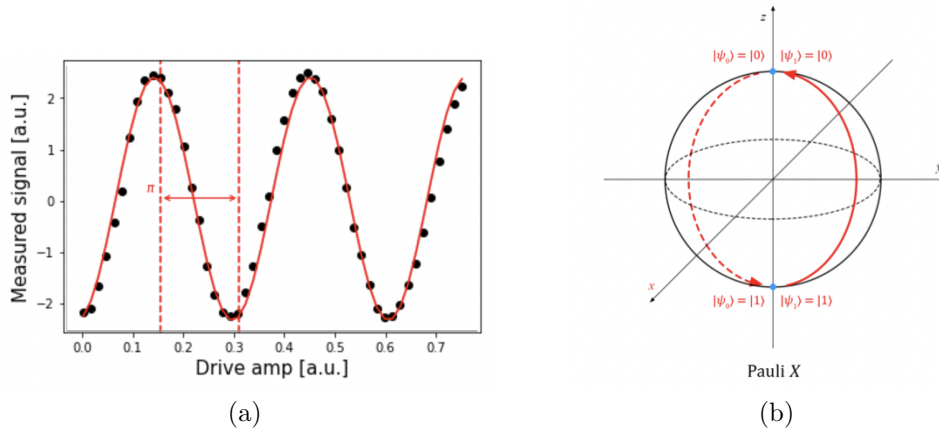


Figure 10: (a) Rabi Oscillations. At each step the state of the qubit is measured for different drive amplitudes. The results were fit (red) by Eq. (8). The  $\pi$  pulse  $t = \frac{\pi}{\omega_1}$  determines the transition between states  $|0\rangle$  and  $|1\rangle$ . (b) Rotation on the Bloch sphere by  $\pi$  radians around the X-axis (applying X-gate) is analogous to applying the  $\pi$  pulse.

### 5.3 0/1 Discriminator

Our task is to create a state  $|1\rangle$  after applying our calibrated  $\pi$  pulse to a qubit in superposition and building a discriminator - a function that takes a measured andkerneled complex value and classifies it as either "0" or "1". By repeatedly doing the experiment and plotting the measured signal we obtain two clusters (Figure 11). They vizualize the results from the ground state in blue and the results from the excited state in red.

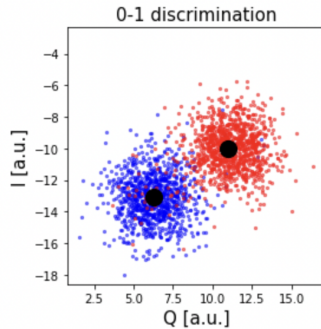


Figure 11: 0/1 Discrimination in the IQ plane. The two clusters represent the two states "0" and "1" in blue and red respectively.

### 5.4 Relaxation time $T_1$

The **relaxation time**  $T_1$  is the time it takes for a qubit to decay from excited to ground state. The experiment uses the  $\pi$  pulse and then we apply a measure pulse after a delay varying between the experiment. The result is a signal that delays exponentially (Figure 13a).

### 5.5 Ramsay Experiment. Precise Qubit Frequency

For a better precision we are using a Ramsey pulse sequence to determine the qubit frequency. An oscillation at the difference in frequency between the applied pulses and the qubit should be observed as we are measuring the signal at the same frequency for both. We will drive the pulses off-resonance by a known amount and the signal oscillations should be with a small offset frequency. The data is then fitted to a sinusoid and we extract the offset frequency  $\Delta f = 2.02MHz$  (Figure 12). The precise qubit frequency is as follows:

$$f = f_{rough} + \Delta f = 4.97166GHz \quad (9)$$

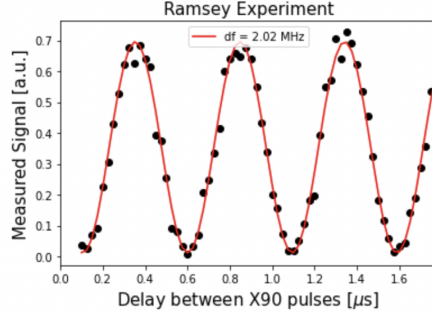


Figure 12: Ramsay Experiment. Ramsay pulse sequence is applied to the qubit: first  $\pi/2$  pulse and after a time delay  $\Delta t$  a second  $\pi/2$  pulse. The pulses are driven off-resonance by a  $f_{detuning} = 2MHz$ . The Ramsey frequency is then the sum of the rough qubit frequency and the detuning frequency. The data is fit to the function  $A\cos(2\pi\Delta fx - C) + B$ . The offset is  $\Delta f = 2.02MHz$

## 5.6 Hahn Echo Experiment. Measuring time $T_2$

The Hahn echo is a pulse sequence similar to the Ramsay experiment, with a  $\pi$  pulse between the two  $\pi/2$  pulses (Figure 13b). The additional pulse applied at time  $\tau$  reverses the accumulation of phase and an echo at time  $2\tau$  is created. The decay time for the experiment gives us the coherence time  $T_2$

$$T_2 = 311.33\mu s \quad (10)$$

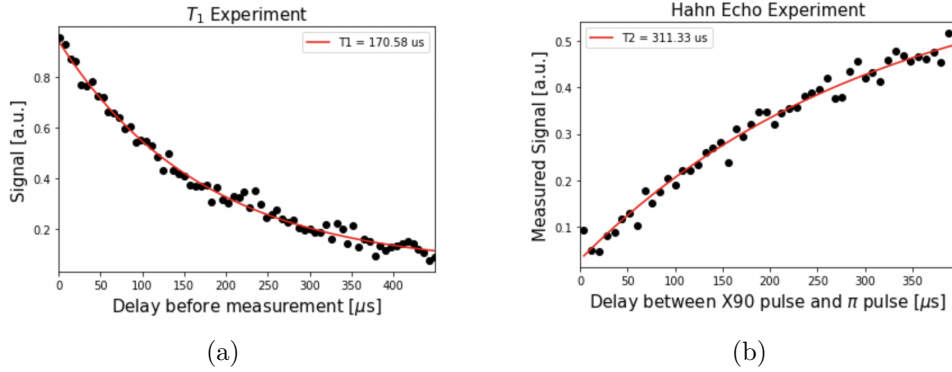


Figure 13: (a) **Relaxation Time Experiment.** The plot shows the measured signal as a function of the delay time. An exponential decay is being observed as the qubit relaxes in energy. The data is fit to a decaying exponential, giving us the time  $T_1$  from the equation  $Ae^{-\frac{x}{T_1}+C}$ ,  $T_1 = 170.58\mu s$ . (b) **Hahn Echo Experiment** for measuring the coherence time  $T_2$  of the qubit. A pulse sequence is being applied as follows:  $\pi/2, \pi(at\ time\ \tau), \pi/2$ . The measured signal is shown as a function of the delay. The decay time  $T_2$  is obtained after fitting the data to  $Ae^{-\frac{x}{T_2}+B}$

## 5.7 Dynamical Decoupling

Dynamical decoupling allows the cancellation of different frequencies of noise and is used to extract longer coherence times from qubits. For the given range in microseconds and after fitting the data, we get:

$$T_{2DD} = 253.67\mu s \quad (11)$$

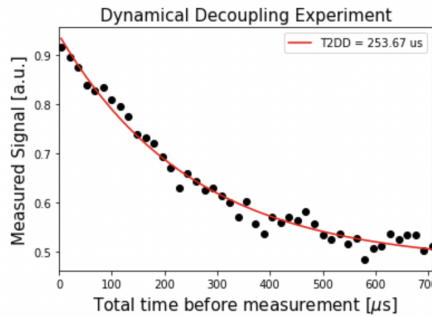


Figure 14: Dynamical Decoupling Experiment. The Hahn experiment was modified by applying several  $\pi$  pulses. Using the fit for the equation  $Ae^{\frac{-x}{T_{2DD}}+B}$  we get the coherence time of  $T_{2DD} = 253.67\mu s$

## 6 Conclusions

The purpose of the project "Introduction to Quantum Computing" was to cover the basics of quantum mechanical phenomena and key concepts in quantum computing technologies.

The first experiment investigated the state transitions of qubits in order to find the resonant frequency. Afterwards, a  $\pi$  pulse was applied periodically, analogous to applying a X-gate to the qubit. As a result Rabi Oscillations were obtained. After fitting the data the amplitude of the  $\pi$  pulse was found. We used the calibrated  $\pi$  pulse to create a state  $|1\rangle$  from a qubit in a superposition and build a discriminator afterwards. The signal from the repeated experiment showed two clusters - one representing the excited state and one - the ground state.

The Ramsay pulse sequence was used to determine the precise qubit frequency by driving the pulses off-resonance by a known amount. With the following experiments the relaxation time  $T_1$  and the coherence time  $T_2$  were found. The final experiment, the Dynamical Decoupling, allows the cancellation of noise and it was used to extract longer coherence times from qubits.

## References

- [1] Chris Bernhardt. *Quantum computing for everyone*. Mit Press, 2019.
- [2] Adem Ergül. *Nonlinear dynamics of josephson junction chains and superconducting resonators*. PhD thesis, KTH Royal Institute of Technology, 2013.
- [3] David J Griffiths. *Introduction to quantum mechanics*. Pearson International Edition (Pearson Prentice Hall, Upper Saddle River, 2005), 1962.
- [4] Jens Koch, M Yu Terri, Jay Gambetta, Andrew A Houck, David Isaac Schuster, Johannes Majer, Alexandre Blais, Michel H Devoret, Steven M Girvin, and Robert J Schoelkopf. Charge-insensitive qubit design derived from the cooper pair box. *Physical Review A*, 76(4):042319, 2007.
- [5] Michel Le Bellac et al. *A short introduction to quantum information and quantum computation*. Cambridge University Press, 2006.
- [6] François Nguyen. *Cooper pair box circuits: two-qubit gate, single-shot readout, and current to frequency conversion*. PhD thesis, Université Pierre et Marie Curie-Paris VI, 2008.
- [7] Robert S Sutor. *Dancing with Qubits: How quantum computing works and how it can change the world*. Packt Publishing Ltd, 2019.